Stable and reliable ohmic contact on p-type 4H-SiC up to 1500 h of aging at 600°C

Valdemar Abou Hamad, Tony Abi Tannous, Maher Soueidan, Laurent Gremillard, Damien Fabrègue, Jose Penuelas, Youssef Zaatar

Stable and reliable ohmic contact on p-type 4H-SiC up to 1500 h of aging at 600°C

Published in Microelectronics reliability 110 (2020) article # 113694

https://doi.org/10.1016/j.microrel.2020.113694

ABOU HAMAD Valdemar[a,b*], ABI TANNOUS Tony[c*], SOUEIDAN Maher[d], GREMILLARD Laurent[b], FABREGUE Damien[b], PENUELAS Jose[e], ZAATAR Youssef[a]

a. Lebanese University, LPA, Faculty of Science, BP 90656 - Jdeidet - Lebanon.
b. Université de Lyon, INSA-Lyon, CNRS, MATEIS, UMR 5510, 20 Avenue Albert Einstein, F-69621 Villeurbanne, France.
c. Université de Lyon, INSA-Lyon, CNRS, Laboratoire Ampère, UMR 5005, F-69621, France.
d. Lebanese National Council for Scientific Research, Lebanese Atomic Energy Commission, P.O. Box 11-8281, Riad El Solh 1107, 2260 Beirut, Lebanon.
e. Institut des Nanotechnologies de Lyon-INL, UMR 5270 CNRS, Université de Lyon, École Centrale de Lyon, 36 avenue Guy de Collongue, F-69134 Ecully cedex, France.

*. Both authors contributed equally to this work.

Corresponding author:
Valdemar ABOU HAMAD
valdemar.ah@hotmail.com

Abstract

The stability and reliability at high temperature of Ti_3SiC_2 based ohmic contacts on p-type 4H-SiC (0001) 4°-off substrates were studied. The contact was grown from $Ti_{100-x}Al_x$ alloys annealed at high temperature (from 900°C to 1200°C). The Specific Contact Resistance (SCR) at room temperature and at high temperature (up to 600°C) was in the 10^{-4}-10^{-5} $\Omega.cm^2$ range. A Schottky barrier height of 0.71 to 0.85 eV was calculated for the set of samples. After aging period at 600°C for 1500h, the SCR was very stable for Al contents x < 80 at%. This was correlated with chemical and physical stability of these contacts, where the residual stress located on 4H-SiC/Ti_3SiC_2 interface decreased after aging, for which the Ti_3SiC_2 phase was preserved. Whereas, in the case of x = 80 at%, the Ti_3SiC_2 phase disappeared and the contacts were not ohmic anymore after long time aging. The obtained results showed that Ti_3SiC_2/4H-SiC system is thermodynamically stable at high temperatures and can therefore be a good candidate, with high potential, for high power and high temperature electronic applications.

Keywords:

Silicon carbide, MAX phase, High temperature, Specific contact resistance.

1 Introduction

The semiconductor 4H-SiC is nowadays reaching maturity in both material growth and device performance aspects. Although, current 4H-SiC electronic devices are applied to work at higher temperature than Si- or GaAs-based counterparts, which are limited to temperatures < ~300°C. But several niche applications require device operation at even higher temperatures (> 300°C), such as space (e.g. Venus exploration) or engine monitoring (HT sensors). In fact, the semiconductor 4H-SiC received a high attention by the modern techniques of material growth in high power electronic components because of its special characteristics and abilities in high temperature applications: namely, a good performance at high temperatures; intense powers and high frequencies [1, 2]. 4H-SiC combines exceptional electronic and physical properties [3], such as, a wide bandgap (about 3 times that of Si) [4], high electron saturation velocity and a low intrinsic carrier concentration at high temperatures, comparing to Si, which improves its ability of voltage blocking [5]. Furthermore, 4H-SiC is characterized by its hardness, its low density and its high thermal conductivity [6, 7]. All these properties and much more give 4H-SiC exceptional qualities in high power and high temperature applications.

Among the various reasons for device failure at high temperature is the reliability of the electrical contacts with 4H-SiC [8-11]. Degradation of the contacts usually comes from enhanced chemical reactivity at high temperature. Thus, changes occur in the chemistry of the phases in direct contact with SiC. Ideally, the materials forming the high temperature electric contacts should be in thermodynamic equilibrium with SiC on a wide temperature range to avoid any chemical evolution. On the other hand, the number of metals or materials that can form an ohmic contact on p-type 4H-SiC, is limited, since it is difficult to find metals with an appropriate work function capable of forming an ohmic contact on p-type 4H-SiC which has a high Schottky barrier height (~7 eV) [12, 13]. To obtain such contact on p-type 4H-SiC, aluminum-based alloys are generally used [14]. Many different alloys have been investigated [15], such as Al-Ti [12], Ti/Al/W [13], Ni/Ti/Al [16], Ti/Al/Si [17]. Thierry-Jebali et al. have reported the formation of Ni/Ti/Al contacts on highly p-type 4H-SiC with low Specific Contact Resistance (SCR = 2.8×10^{-6} $\Omega\cdot cm^2$), but this result was not reproducible [18]. Another study reported the formation of contacts on highly p-type 4H-SiC after annealing at 800ºC (relatively low temperature) for 30 min, but such long annealing time can be detrimental for MOSFET fabrication process [19]. On the other hand, a great attention is given to Al-Ti alloy which has shown stable low SCRs on the order of 10^{-3}–10^{-5} $\Omega\cdot cm^2$ on p-type SiC [20, 21]. The formation of the $M_{n+1}AX_n$ phase Ti_3SiC_2, after annealing of Al–Ti alloy at high temperature, is the reason behind the stability of the ohmic contact on p-type 4H-SiC [12, 22, 23].

The ternary group $M_{n+1}AX_n$ phases (n = 1, 2 or 3) holds its name from its chemical composition, where M is an early transition metal, A is an A-group element (mostly IIIA and IVA) and X is either C and/or N [24-28]. This group of materials combines both metallic and ceramic characteristics: namely, good electrical and thermal conductivity (Metallic properties); good resistance to oxidation and corrosion (Ceramic properties) [29, 30]. Among the MAX phases, Ti_3SiC_2 is a promising material for such high temperature contacts since it is a thermally stable compound which does not react with 4H-SiC at temperatures up to 1200°C and has a Coefficient of Thermal Expansion (CTE) close to that of 4H-SiC [31]. Furthermore, it was shown that this material can lead to low contact resistivity on p-type 4H-SiC [22, 32, 33], which is known to be more difficult than for n-type case. The lowest contact resistivity is obtained when forming Ti_3SiC_2 epitaxial to 4H-SiC (0001) by annealing Al-Ti based alloys [22, 32, 33]. To the best of our knowledge, the high temperature (>300°C) stability and reliability of these contacts have never been investigated. Therefore, an electrical analysis was done using the Transfer Length Method (TLM) to calculate the contact resistivity at high temperatures. In addition, the strain present in the 4H-SiC/Ti_3SiC_2 interface, is estimated with Williamson-Hall analysis (W-H). Afterwards, X-ray Reciprocal Space Mapping (RSM) is applied on 4H-

SiC/Ti_3SiC_2 samples, in order to study the structural properties of the thin film before and after aging, with a particular attention to the epitaxial interface. This is the aim of the present work for which the targeted test temperature was set as high as 600°C.

2 Experimental

2.1 Sample synthesis

P-type doped epitaxial layers (~1.3 μm thick, [Al] ~ [1-4] × 10^{19} cm^{-3}) on 4H-SiC (0001) 4° off substrates were used in this study. The samples were cleaned using acetone and ethanol ultrasonic degreasing, for 5 min each. It was followed by acid treatments: 10 min H_2SO_4:H_2O_2 (2:1) then 4 min HF 5% diluted. Finally, the samples were rinsed with deionized water, and blown dry with N_2 gun. Electrical insulation of the p type layers was done by forming mesa structures using reactive-ion etching (RIE) in an Alcatel Nextral NE110 reactor during 7 min at 60 mtorr under SF_6 (25 sccm) and O_2 (7 sccm) and a RF power of 250 W. After RIE, the samples underwent a second chemical cleaning as mentioned above. Then, 200 nm films of $Ti_{100-x}Al_x$ (50 at% ≤ x ≤ 80 at%) were deposited at room temperature by magnetron sputtering from three different alloy targets of $Ti_{100-x}Al_x$ composition, with an Ar constant pressure of ~5×10^{-3} mbar (Figure 1). The film's composition was determined and checked using Energy Dispersive Spectrometry (EDS).

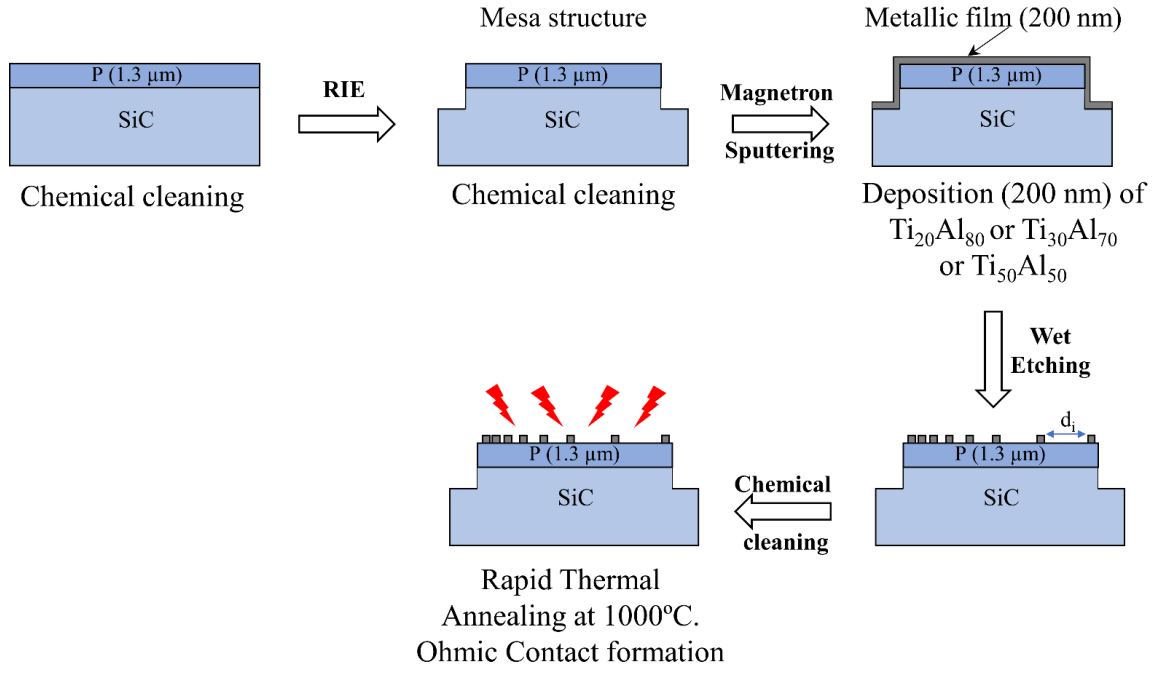

Figure 1: Schematic showing the sample synthesis of Al-Ti-based contact on p-type 4H-SiC, and TLM structure preparation.

2.2 TLM structure preparation

Transfer Length Method (TLM) structures were then fabricated on the mesa, in order to determine the electrical properties of the metal/p-type 4H-SiC contact. This was performed by standard photolithography followed by wet etching using commercial Al-etch at 60°C. The TLM pattern was composed of seven rectangular electrodes (500 × 100 μm^2) with increasing spacings of 3, 6, 10, 20, 40, 80, and 120 μm. For ohmic contact formation, rapid thermal

annealing (RTA) of the $Ti_{100-x}Al_x$ alloys was performed under argon at atmospheric pressure. The heating rate was 20°C/s and the annealing plateau was set to 1000°C for 10 min as these conditions were found to give the best results in terms of contact resistivity (SCR = 9.8×10^{-6} $\Omega\cdot cm^2$ at 600ºC, according to ref [32]). After optical microscopy inspection of the annealed TLM patterns, we could confirm that their dimensions and the interpad distances did not change so that no correction was needed during the TLM measurements. Note that the length of the rectangular pads, 500 μm, is large enough compared to the distance between the pads and to the distance between the pads and the edge of the mesa (5 μm), so that the current crowding effect can be considered negligible.
The structural properties of the contacts were routinely determined by X-ray diffraction (XRD) on a 'Rigaku Smartlab' diffractometer equipped with a Cu rotating anode working at 9 kW, and the wavelength was set to λ = 1.54056 Å. The electrical characterization was done using a Keithley source measurement unit K2602A, where the samples are mounted directly on a heating chuck of a probe station. They are characterized at different temperature, up to 600°C, and monitored using a K-type thermocouple. The temperature accuracy of the tests was of ±1%. Above 300°C, electrical tests are performed under vacuum to prevent oxidation of the TLM structures. A four-probe setup is used (Kelvin configuration) to eliminate cable and tips resistances, which results in a measurement accuracy value better than 1%. *I–V* characteristics are plotted as a function of the contact spacing of different temperatures.

2.3 Aging conditions

To study the reliability of these contacts, the aging conditions were 600°C under pure argon (not under air, to prevent oxidation of Al at surface) for durations up to 1500 h. These aging tests were carried out in a resistively heated tubular furnace. The evolution of contact nature and resistivity was determined after each aging period intervals (24, 48, 100, 200, 400, 700, 1000 and 1500 h) using the following procedure: 1) the samples were cooled down to room temperature, then 2) they underwent XRD analyses and contact resistivity measurements after which 3) they were put back in the aging furnace and heated again to 600°C for the subsequent aging interval.

3 Results and discussion

3.1 Specific contact resistance

For $Ti_{20}Al_{80}$–based contact, the evolution of the specific contact resistance (SCR) as a function of aging time is shown in Figure 2 (black points). It was found to decrease from 4.1×10^{-4} to 2.1×10^{-4} $\Omega.cm^2$ within the first 48 h of aging. For longer aging time, the I-V characteristics were not linear anymore which means that the contact became non-ohmic. When looking to the XRD patterns recorded before and after 100 h of aging, one note that the ohmicity degradation could be correlated to compositional changes of the metallic phases present in the contact (Figure 3). Indeed, after aging the diffraction peaks corresponding to Al and Ti_3SiC_2 almost disappeared while the intensity of the Al_3Ti peaks increased. As a matter of fact, the ohmicity loss can be correlated to the disappearance of the Ti_3SiC_2 phase.

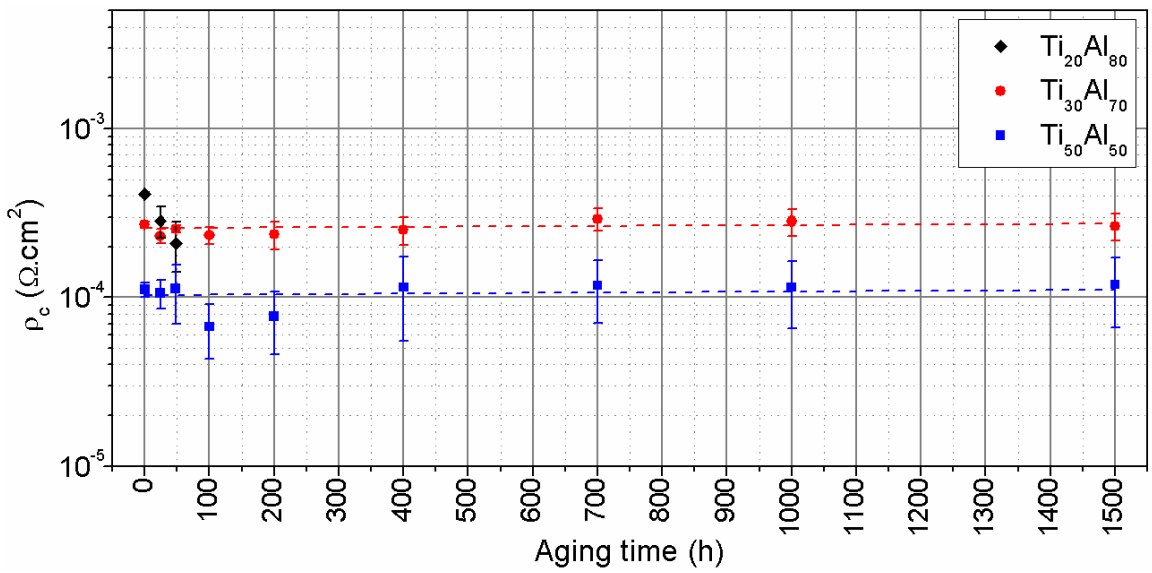

Figure 2: Variation of the SCR as a function of aging time for Ti20Al80, Ti30Al70 and Ti50Al50-based contacts.

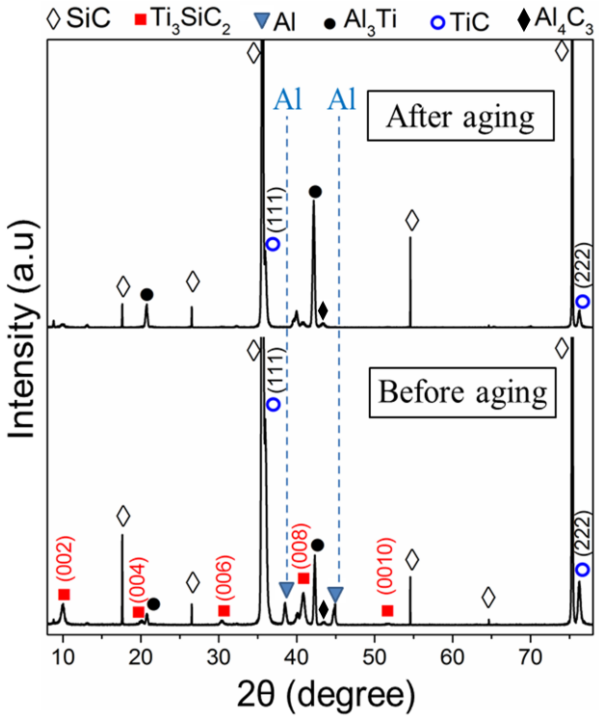

Figure 3: XRD patterns before and after aging of Ti20Al80-based contact.

This is not the case for $Ti_{30}Al_{70}$ and $Ti_{50}Al_{50}$-based contacts for which the SCR kept constant even after 1500 h of aging at 600°C (Figure 2). When looking to the corresponding XRD patterns of $Ti_{50}Al_{50}$-based contacts in Figure 4, it is obvious that only the Al peaks disappeared after aging, while the ones of Ti_3SiC_2 were still present, though of lower intensity. Also, less obvious but detectable is the evolution of Al_3Ti peaks: they increased while shifting towards low angles. This is better seen in Figure 5, for which the XRD patterns were recorded after only 24 h of aging. In fact, these few changes in the contacts composition seems to happen during

the early aging time (≤ 24 h) while after that no further change is observed. We can therefore conclude that the system reaches a thermodynamic stability in the first aging hours.

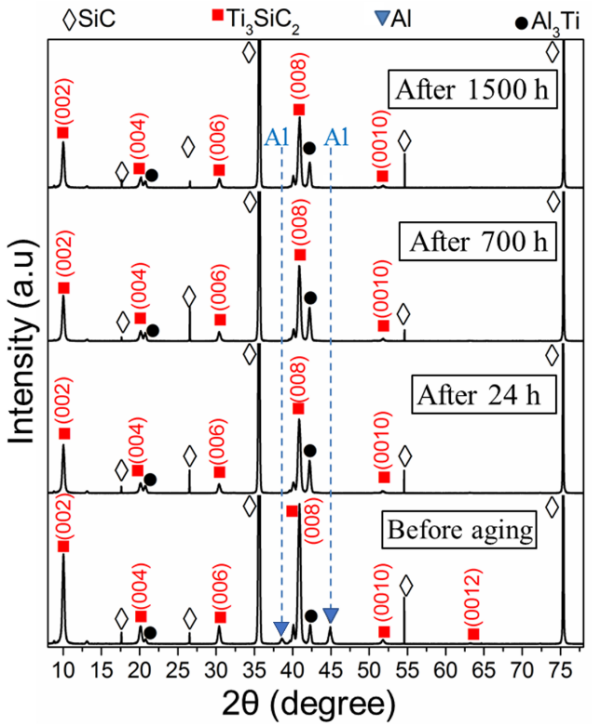

Figure 4: XRD patterns before and after different aging times of $Ti_{50}Al_{50}$-based contacts.

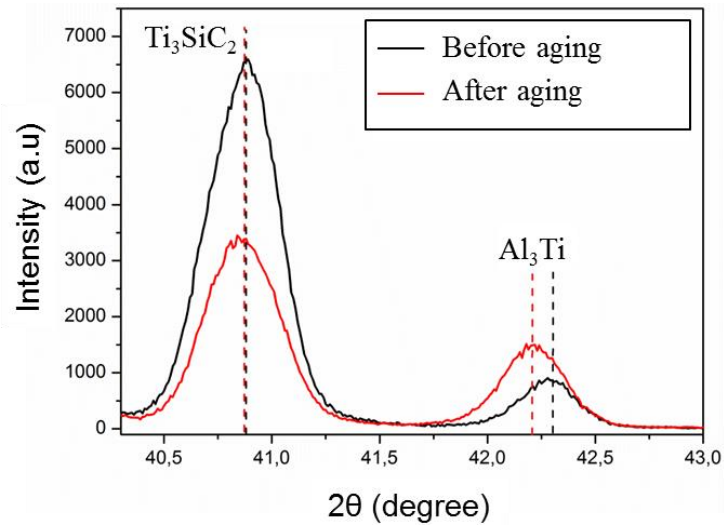

Figure 5: Zoom on the XRD pattern recorded for $Ti_{50}Al_{50}$-based contact, before and after 24 hours of aging at 600°C. Note after aging the decrease of the Ti_3SiC_2 peak intensity and the increase and shift, to lower angles, of the Al_3Ti peak.

Many investigations focused on the thermal stability of ohmic contacts on p-type 4H-SiC at high operating temperatures up to 600ºC. A reported Ni/Ti/Al ohmic contacts on p-type 4H-SiC showed significant changes in the contact resistivities and an electrical degradation after aging at 600ºC for 100h [16]. Vivona et al. have reported the thermal stability of Ti/Al/W

contacts to p-type implanted 4H-SiC at 400ºC, and the results showed some changes in the contact resistivity after 100h of aging [13]. Furthermore, recent studies presented the thermal stability of Ti/Pt, Ni/Ti/Ni/$TaSi_2$/Pt and Ni/W/$TaSi_2$/Pt contacts to p-type implanted 4H-SiC at 500ºC for 300h [34, 35]. The SCR of Ti/Pt increased dramatically to 2 $\Omega \cdot cm^2$ after 200h of aging at 500ºC [34]. In addition, the SCR value of Ni/Ti/Ni/$TaSi_2$/Pt contact on p-type 4H-SiC increased in the initial 50h of aging at 500ºC [34]. Moreover, the reported Ni/W/$TaSi_2$/Pt ohmic contact on p-type 4H-SiC showed some changes in the SCR on the order of 10^{-3} $\Omega \cdot cm^2$ after 300h of aging at 500ºC [35]. On the other hand, the results presented in Figure 2, of this study, showed an extreme electrical stability for $Ti_{30}Al_{70}$ and $Ti_{50}Al_{50}$-based contacts where the SCR kept constant at 600°C even after 1500h, which is relatively a long time of aging. The obtained results demonstrated the reliability and the thermal and electrical stability of $Ti_{30}Al_{70}$ and $Ti_{50}Al_{50}$-based contacts on p-type 4H-SiC, which is promising for high temperature applications.

3.2 Chemical analysis

As a matter of fact, for all the samples of this study, the observed phases evolution after aging is rather similar:

- Pure Al phase disappears
- Ti_3SiC_2 phase amount decreases
- Al_3Ti phase amount increases

Based on these results, we can propose that the following reaction takes place during the aging at 600°C:

$$Ti_3SiC_2 + 9Al \rightarrow 3Al_3Ti + SiC + C \qquad (1)$$

This reaction is obviously not complete in the case of $Ti_{30}Al_{70}$ and $Ti_{50}Al_{50}$-based contacts since Ti_3SiC_2 phase is still detected in these samples, even after 1500 h of aging. This is probably due to the exhaustion of elemental Al which stops the reaction. But, such reaction does not explain the low-angle shift of Al_3Ti peak after aging. The literature mentions that Al_3Ti can contain up to 15% at. of Si in its lattice, forming a $(Al\text{-}Si)_3Ti$ solid solution [36] and shifting its XRD peaks to low angles. Assuming the formation of such solid solution, we can rewrite equation (1) as follows:

$$Ti_3SiC_2 + 9(1-x)Al \rightarrow 3(Al_{1-x}Si_x)_3Ti + (1-9x)SiC + (1+9x)C \qquad (2)$$

It is interesting to compare these reactions to the one proposed in [37] for the formation of Ti_3SiC_2 during the 1000°C rapid thermal annealing:

$$20Al + 9Ti + 2SiC \rightarrow Ti_3SiC_2 + 6Al_3Ti + 2Al + Si \qquad (3)$$

Obviously, reaction (3) cannot be considered as the reverse of reactions (1) or (2). According to ref [38], annealing an Al-rich Al-Ti alloy on SiC at 700°C leads to the only formation of Al_3Ti phase, almost without Ti_3SiC_2. As a matter of fact, Al_3Ti seems to be the equilibrium phase with SiC at low temperature ($\leq$ ~700°C), while this equilibrium shifts toward Ti_3SiC_2 formation at higher temperatures. Assuming this, we can now explain the chemical evolution of the contacts after aging at 600°C: such lower temperature treatment provokes the displacement toward Al_3Ti phase of the equilibrium with SiC, at the expanse of Ti_3SiC_2 phase. Due to some probable loss of Al (by evaporation) during the various annealings, reaction (2) is not complete so that the system does not shift completely to the equilibrium with Al_3Ti and then both Ti_3SiC_2 and Al_3Ti phases coexist. The important consequence of such incomplete reaction is that the contact is in thermodynamic equilibrium with SiC as long as no Al is added to the system. It means that, as long as only chemical reactivity is governing the contacts ohmicity, this contact can virtually remain perfectly stable at 600°C, no matter the aging time.

Finally, note that both reactions (1) and (2) should lead to the formation of SiC and C. Unfortunately, we could not confirm this point since the XRD spectra did not display evidence of these phases. Further analyses are programmed to evidence the possible presence of elemental carbon, such as Raman spectroscopy or cross-section elemental analyses. But in all cases, these extra phases do not seem to be detrimental to the contact stability and thus no visible impact on the overall thermodynamic equilibrium is detected.

3.3 Strain and Stress

In the following, we used the Williamson-Hall (W-H) method to investigate the origin of the X-ray diffraction peaks broadening. It is obvious from equation (5) that the corrected peak broadening β_{hkl} (in radians) varies as $1/\cos\theta$ from crystallite size (L) and as $\tan\theta$ from strain (ε). The W-H method consists on separating the size and strain broadening by presenting the peak width as a function of the diffracting angle 2θ, giving the following equation:

$$\beta_{hkl} = \beta_L + \beta_s \qquad (4)$$

$$\beta_{hkl} = \frac{k\lambda}{L\ cos\theta} + (4\varepsilon \tan\theta) \qquad (5)$$

By rearranging Eq. (5):

$$\beta_{hkl} \cos\theta = \frac{k\lambda}{L} + 4\varepsilon \sin\theta \qquad (6)$$

Two graphs were plotted for $Ti_{50}Al_{50}$-based contacts before and after aging up to 1500h at 600ºC, with '$4\sin\theta$' defining the x-axis and '$\beta_{hkl}\cos\theta$' defining the y-axis. The plots are illustrated using the preferred orientation peaks of Ti_3SiC_2. Afterwards, a linear fit is applied on the plots, and the strain is determined from the slope of the fit. Figure 6 shows the W-H plots for Ti_3SiC_2-based contacts before and after aging up to 1500h at 600ºC. It is remarkable that the strain in the Ti_3SiC_2 thin film before aging is larger than after aging, meaning that aging has an effect on the strain located in the contact. In addition, the stress exerted on the contact can be determined by using the generalized Hooke's law $\sigma = E \cdot \varepsilon$, where the linear proportionality between stress(σ) and strain(ε) is considered, with Young's modulus (E = 326GPa for Ti_3SiC_2 [39]) being the constant of proportionality. As result, the stress exerted on Ti_3SiC_2-based contact has reduced from 145MPa to 11MPa which means that the stress in the contact has almost totally relaxed after being subjected to a temperature of 600ºC up to 1500h, and no serious deformation or damage have occurred in the physical structure of the contact.

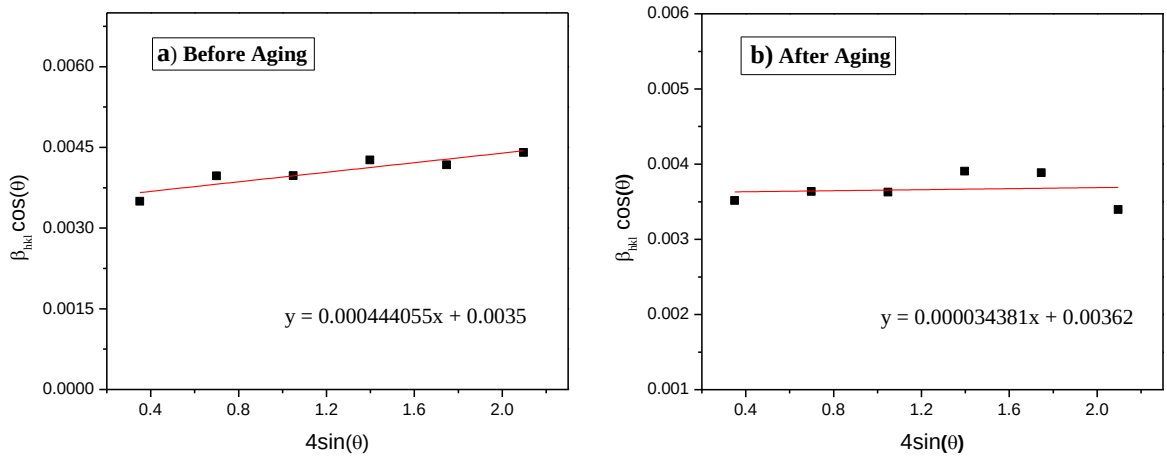

Figure 6: W-H analysis of $Ti_{50}Al_{50}$-based contacts, a) Before aging, b) After aging up to 1500h at 600ºC.

3.4 Reciprocal space mapping

Figure 7 illustrates the RSM patterns around 4H-SiC (1 0 7) and Ti_3SiC_2 (1 0 12), which were used to determine the d-spacing for each phase. Because of the hexagonal structure of 4H-SiC and Ti_3SiC_2, the lattice parameter 'a' was calculated by the following equation [40]:

$$\frac{1}{d^2} = \frac{4}{3}\left(\frac{h^2+hk+k^2}{a^2}\right) + \frac{l^2}{c^2} \qquad (7)$$

The obtained results are presented in Table 1.

Table 1: Lattice parameters.

	Lattice parameter (Å)		
	Theoretical value	**Before aging**	**After aging**
4H-SiC (1 0 7)	a = 3.079 c = 10.061	a = 3.079 c = 10.061	a = 3.079 c = 10.061
Ti_3SiC_2 (1 0 12)	a = 3.068 c = 17.669	a = 3.079 c = 17.656	a = 3.069 c = 17.667

Table 1 shows that the calculated lattice parameter a = 3.079Å of 4H-SiC is equal to the theoretical value, which is 3.079Å and didn't change before and after aging. Besides, it is remarkable that for Ti_3SiC_2, before aging the parameter 'a' is equal to that of 4H-SiC which means it is larger than the theoretical value a = 3.068Å. Therefore, due to the difference between the theoretical and the calculated value of the lattice parameter of Ti_3SiC_2, stress was introduced into the contact. On the other hand, after aging the lattice parameter 'a' of Ti_3SiC_2 reduced (a = 3.069 Å) and reached a closer value to the theoretical one (a = 3.068 Å), leading to a stress relaxation in the Ti_3SiC_2-based contact.

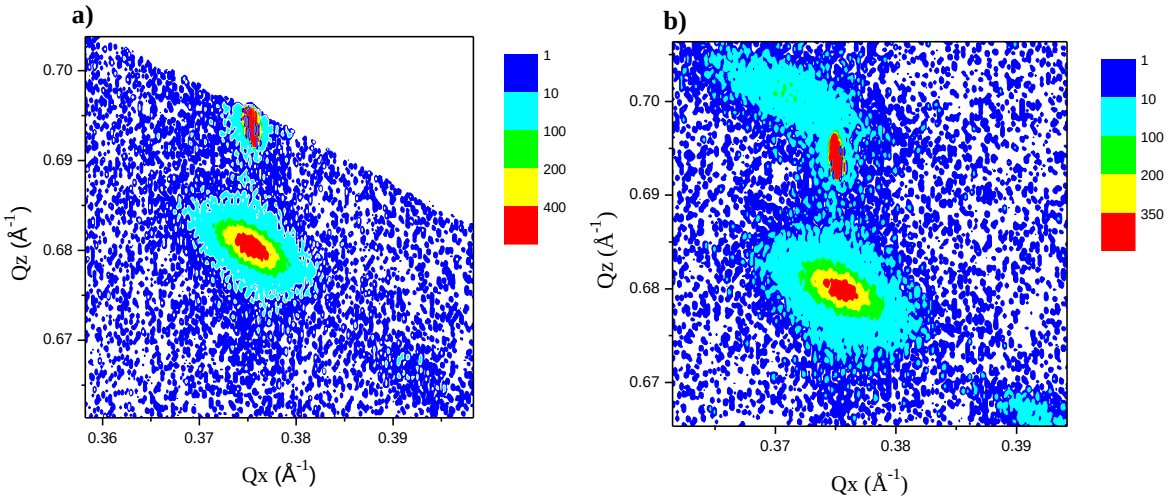

Figure 7: Reciprocal space maps around SiC (1 0 7) and Ti_3SiC_2 (1 0 12), a) Before aging, b) After aging.

In brief, the synthesized layer of Ti_3SiC_2 adopted a lattice parameter equal to that of the 4H-SiC substrate, which caused some strain in the Ti_3SiC_2 layer. However, the aging at 600°C for 1500h permitted the Ti_3SiC_2 layer to reach a lattice parameter closer to the normal one of the Ti_3SiC_2 phase. The obtained results showed that the strain and the stress exerted on Ti_3SiC_2-based contact reduced after aging, this means there is no serious structural deformation occurring to the Ti_3SiC_2 layer, consequently 4H-SiC/Ti_3SiC_2 interface is intact. The good mechanical behavior and the physical constancy of the contact could be one of the reasons that improve the reliability of the contact, and leading to a low and stable electrical resistivity even at high temperatures.

Conclusion

In this paper, an electrical study was done using Transfer Length Method (TLM) to calculate the specific contact resistance of Ti_3SiC_2-based contact formed on a 4H-SiC p-type substrate. The TLM was applied on the samples before and after aging for 1500h at 600ºC. In addition, strain, stress and lattice parameters located in Ti_3SiC_2 thin films were determined in order to examine the effects of high temperature on the physical structure of the electrical contact and 4H-SiC/Ti_3SiC_2 interface. In conclusion, Al-Ti based metallization on p-type 4H-SiC allows elaborating low resistivity and reliable contacts for operating temperatures as high as 600°C. This can be achieved for an initial Al content in the 50 - 70 at% range which produces the suitable 4H-SiC/Ti_3SiC_2 interface which is not converted back to Al_3Ti upon aging at 600°C for up to 1500h. Besides, mechanical stress, exerted on the electrical contact, decreased after aging, which is leading to a relaxation in the contact and preventing a serious structural deformation. The physical stability helps the contact to keep a steady resistivity, as well as the chemical balance. Such interface is thermodynamically stable and can thus virtually remain perfectly stable and reliable at temperatures up to 600°C.

References

[1] Tony Abi Tannous. 'Nouveaux contacts électriques sur SiC-4H de type p à base de carbure Ti3SiC2'. Journées. JCGE'2014 - SEEDS, Jun 2014, Saint-Louis, France.

[2] J.B. Casady, R.W. Johnson, 'Status of silicon carbide (SiC) as a wide-bandgap semiconductor for high-temperature applications: A Review', Solid-State Electron. 39(10), (1996), 1409-1422.

[3] T. Kimoto, J.A. Cooper. Fundamentals of Silicon Carbide Technology: Growth, Characterization, Devices and Applications, John Wiley & Sons, Singapore, (2014).

[4] H. Fashandi et al. 'Single-step synthesis process of Ti3SiC2 ohmic contacts on 4H-SiC by sputter-deposition of Ti'. Scripta Materialia, 99 (2015), 53–56.

[5] C. Raynaud et al. Comparison of high voltage and high temperature performances of wide bandgap semiconductors for vertical power devices. Diamond & Related Materials. Vol.19, (2010), pp.1–6.

[6] K. Strecker, S. Ribeiro, R. Oberacker, M.-J. Hoffmann. Influence of microstructural variation on fracture toughness of LPS-SiC ceramics. International Journal of Refractory Metals and Hard Materials, 22(4-5), (2004), 169–175.

[7] Robert F. Davis, "Silicon Carbide". Reference Module in Materials Science and Materials Engineering. vol. 13, (2017), pp. 1–10.

[8] L.M. Porter, and R.F. Davis, 'A critical review of ohmic and rectifying contacts for silicon carbide'. Meter. Sci. Eng. B, 34, 83 (1995).

[9] R.Wenzel, F. Goesmann, R. Schmid-Fetzer. Proceedings of the high temperature Electronic Materials, Devices and sensors conference, San Diego, CA, (1998), p. 159.

[10] S. Liu, K. Reinhardt, C. Servert, J. Scofield, M. Ramalingam, C. Tunstall, Proceedings of the 3rd International High Temperature Electronics Conference, Alburquerque, NM, (1996), p. 9.

[11] N.A. Papanicolaou, A.E. Edwards, M.V. Rao, A.E. Wickenden, D.D. Koleske, R.L. Henry, W.T. Anderson, Proceedings of the 4th International High Temperature Electronics conference, Alburquerque, NM, (1998), p. 122.

[12] F. Roccaforte, A. Frazzetto, G. Greco, F. Giannazzo, P. Fiorenza, R. Lo Nigro, M. Saggio, M. Leszczynski, P. Pristawko, V. Raineri, 'Critical issues for interfaces to p-type SiC and GaN in power devices'. Appl. Surf. Sci. 258, (2012), 8324-8333.

[13] Vivona, M., Greco, G., Lo Nigro, R., Bongiorno, C., & Roccaforte, F. Ti/Al/W Ohmic contacts to p-type implanted 4H-SiC. Journal of Applied Physics, 118(3), (2015), 035705.

[14] Y. B. Luo, F. Yan, K. Tone, J. H. Zhao, and J. Crofton, "Searching for device processing compatible ohmic contacts to implanted p-type 4H-SiC," Mater. Sci. Forum, vols. 338–342, (2000), pp. 1013–1016.

[15] Huang, L., Xia, M., & Gu, X. A critical review of theory and progress in Ohmic contacts to p-type SiC. Journal of Crystal Growth, 531, (2020), 125353.

[16] Yu, H., Zhang, X., Shen, H., Tang, Y., Bai, Y., Wu, Y., … Liu, X. Thermal stability of Ni/Ti/Al ohmic contacts to p-type 4H-SiC. Journal of Applied Physics, 117(2), (2015), 025703.

[17] H. Tamaso, S. Yamada, H. Kitabayashi, and T. Horii, 'Ti/Al/Si Ohmic Contacts for Both n-Type and p-Type 4H-SiC'. Mater. Sci. Forum, 778–780, (2014), 669-672.

[18] N. Thierry-Jebali et al., "Very low specific contact resistance measurements made on a highly p-type doped 4H-SiC layer selectively grown by vapor-liquid-solid transport," Appl. Phys. Lett., vol. 102, no. 21, (2013), pp. 212108-1–212108-4.

[19] S. Tsukimoto, T. Sakai, T. Onishi, K. Ito, and M. Murakami, 'Simultaneous Formation of p- and n-Type Ohmic Contacts to 4H-SiC Using the Ternary Ni/Ti/Al System'. J. Electron. Mater. 34(10), (2005), 1310-1312.

[20] Mohammad, F. A., Cao, Y., Chang, K.-C., & Porter, L. M. Comparison of Pt-Based Ohmic Contacts with Ti–Al Ohmic Contacts for p-Type SiC. Japanese Journal of Applied Physics, 44(8), (2005), 5933–5938.
[21] Roccaforte, F., Vivona, M., Greco, G., Lo Nigro, R., Giannazzo, F., Di Franco, S., Saggio, M. 'Ti/Al-based contacts to p-type SiC and GaN for power device applications'. Physica Status Solidi (a), 214(4), (2016), 1600357.
[22] S. Tsukimoto, K. Ito, Z. Wang, M. Saito, Y. Ikuhara, and M. Murakami, "Growth and Microstructure of Epitaxial Ti_3SiC_2 Contact Layers on SiC". Mater. Trans. 50, (2009), 1071–1075.
[23] K. Buchholt et al., "Ohmic contact properties of magnetron sputtered Ti_3SiC_2 on n- and p-type 4H-silicon carbide," Appl. Phys. Lett., vol. 98, no. 4, pp. 042108-1–042108-3, Jan. (2011).
[24] W. Jeitschko and H. Nowotny, Monatsh. Fur Chem. 98, (1967), 329-337.
[25] W. Jeitschko and H. Nowotny, Monatsh. Fur Chem. 94, (1963), 1198-1200.
[26] O. Beckmann, H. Boller and H. Nowotny, Monatsh. fur Chem. 99, (1968), 1581.
[27] M.A. Pietzka and J.C. Schuster, 'Summary of constitutional data on the Aluminum-Carbon-Titanium system', J. Phase Equilibria. 15, (1994), 392-400.
[28] A.T. Procopio, T. El-Raghy and M.W. Barsoum, 'Synthesis of Ti_4AlN_3 and Phase Equilibria in the Ti-Al-N System', Met. Mater. Trans A. 31A, (2000), 373.
[29] P. Eklund et al. "The $M_{n+1}AX_n$ phases: Materials science and thin-film processing", Thin Solid Films, 518, (2010), 1851.
[30] J.J. Hu, J.E. Bultman, S. Patton, J.S. Zabinski, 'Pulsed Laser Deposition and Properties of $M_{n+1}AX_n$ Phase Formulated Ti_3SiC_2 Thin Films'. Tribol. Lett. 16, (2004), 113-122.
[31] L.H. Ho-Duc, Synthesis and characterization of the properties of Ti_3SiC_2/SiC and Ti_3SiC_2/TiC composites, thesis at Drexel University (2002).
[32] T. Abi-Tannous, M. Soueidan, G. Ferro, M. Lazar, C. Raynaud, B. Toury, M.F. Beaufort, J.F. Barbot, O. Dezellus, and D. Planson, 'A Study on the Temperature of Ohmic Contact to p-Type SiC Based on Ti_3SiC_2 Phase'. IEEE Trans. Electron Devices 63, (2016), 2462-2468.
[33] A. Drevin-Bazin, J.F. Barbot, M. Alkazaz, T. Cabioch, and M.F. Beaufort, 'Epitaxial growth of Ti_3SiC_2 thin films with basal planes parallel or orthogonal to the surface on α-SiC'. Appl. Phys. Lett. 101, 021606, (2012).
[34] Zhang, Y., Guo, T., Tang, X., Yang, J., He, Y., & Zhang, Y. Thermal stability study of n-type and p-type ohmic contacts simultaneously formed on 4H-SiC. Journal of Alloys and Compounds, 731, (2018), 1267–1274.
[35] Li, Y. L., Zhang, Y. M., Tang, X. Y., Guo, T., & Zhang, Y. M. Extremely Thermal Stable Ni/W/$TaSi_2$/Pt Simultaneous Ohmic Contacts to n-Type and p-Type 4H-SiC. Materials Science Forum, 924, (2018), 401–404.
[36] A. Raman and K. Schubert, Z. Mettal. 56, (1965), 44.
[37] T. Abi-Tannous, M. Soueidan, G. Ferro, M. Lazar, B. Toury, M.F. Beaufort, J.F. Barbot, J. Penulas, and D. Planson, 'Parametric investigation of the formation of epitaxial Ti_3SiC_2 on 4H-SiC from Al-Ti annealing'. Appl. Surf. Sci. 347, (2015), 186-192.
[38] Ideguchi, K., Maeda, M., & Takahashi, Y. Nucleation and growth of Ti_3SiC_2 on SiC by interfacial reaction. IOP Conference Series: Materials Science and Engineering, 61, 012032, (2014).
[39] M. W. Barsoum and T. El-Raghy. 'Synthesis and Characterization of a Remarkable Ceramic: Ti_3SiC_2'. J. Am. Ceram. Soc, 79 (7), (1996), 1953-1956.
[40] Suryanarayana C., Norton M.G. Crystal Structure Determination. II: Hexagonal Structures. In: X-Ray Diffraction. (1998), Springer, Boston, MA.